A Smart Sensor Web for Ocean Observation: Fixed and Mobile Platforms, Integrated Acoustics, Satellites and Predictive Modeling

Bruce M. Howe[1], *Member, IEEE*, Yi Chao[2,3], Payman Arabshahi[4] *Senior Member, IEEE*,

Sumit Roy[5], *Fellow, IEEE*, Tim McGinnis[4], Andrew Gray[5]

[1]Department of Ocean and Resources Engineering, University of Hawaii at Manoa, Honolulu, HI 96822

[2]Jet Propulsion Laboratory, California Institute of Technology, Pasadena, California 91109

[3]Joint Institute for Regional Earth System Science and Engineering, University of California, Los Angeles, California 90095

[4]Applied Physics Laboratory, University of Washington, Seattle, WA, 98105

[5]Department of Electrical Engineering, University of Washington, Seattle, WA 98195

Abstract – **In many areas of Earth science, including climate change research and operational oceanography, there is a need for near real-time integration of data from heterogeneous and spatially distributed sensors, in particular in-situ and space-based sensors. The data integration, as provided by a smart sensor web, enables numerous improvements, namely, 1) adaptive sampling for more efficient use of expensive space-based and in situ sensing assets, 2) higher fidelity information gathering from data sources through integration of complementary data sets, and 3) improved sensor calibration. Our ocean-observing smart sensor web presented herein is composed of both mobile and fixed underwater in-situ ocean sensing assets and Earth Observing System satellite sensors providing larger-scale sensing. An acoustic communications network forms a critical link in the web, facilitating adaptive sampling and calibration. We report on the development of various elements of this smart sensor web, including (a) a cable-connected mooring system with a profiler under real-time control with inductive battery charging; (b) a glider with integrated acoustic communications and broadband receiving capability; (c) an integrated acoustic navigation and communication network; (d) satellite sensor elements; and (e) a predictive model via the Regional Ocean Modeling System interacting with satellite sensor control.**

I. Introduction

Earth's oceans are under sampled and efforts are underway to rectify this situation. On global scales, the Integrated Ocean Observing System (IOOS) within the Global Earth Observation System of Systems (GEOSS) is in the process of bringing together satellite, in situ observations, and modeling to provide products on various time and space scales. Satellite observations include sea surface height altimetry for heat content and near surface currents, scatterometry for wind speed and direction, and infrared radiometers for sea surface temperature. In situ elements include a near-global distribution of Argo profiling floats to provide sparse (incoherent, 300 km spacing) in-situ temperature and salinity data, volunteer observing ships (typically temperature profile data), and arrays of moorings, e.g., the TAO-TRITON array in the equatorial Pacific primarily for El Nino monitoring. Numerical modeling is just now reaching the state of being able to assimilate with adequate resolution the satellite altimetry and in situ data, to produce a 4-dimensional ocean state that is dynamically consistent. However, there are still major discrepancies when one looks at the total heat and fresh water budget [1] – various models and independent data driven results for the fraction of sea level rise attributable to ocean thermal expansion and to ice melting are inconsistent within their respective formal error bars. Even just for ocean heat content change, different analysis groups produce estimates that differ by more than the formal error bars, with a spread that is about half the nominal change in heat content over the last 5 decades [2,3]. In a research-oriented effort, the National Science Foundation (NSF) has initiated the Ocean Observatories Initiative (OOI) to provide leading edge infrastructure for long-term sustained observations at a few selected sites. There are many other efforts to develop and sustain long-term ocean observing capability, to complement the satellite data collected by NASA and other space based Earth observing systems.

We are developing a smart sensor web that combines many of the essential elements of an ocean observing system: a mix of fixed and mobile in-situ sensors and satellite sensors that together can perform a combination of spatial and temporal sampling; and an ocean model, embodying all our best and current knowledge of the physics, embedded in a data assimilation framework, that can be used in an adaptive sampling mode to jointly optimize sampling and resource allocation for improved science data [4,5,6]. For all the pieces to work together, the power, communications, and timing network infrastructure must be in place, linking the web between the in-situ and space-based sensors. (We note the field of smart sensor webs is developing and definitions thereof vary.)

Constructing and demonstrating such a sensor web is a major task, and is only possible by building on the efforts of several complementary projects: (a) cabled, profiler mooring (the ALOHA-MARS Mooring (AMM) system)

intended for the NSF OOI, (b) acoustic Seagliders with integrated sensors and modems talking to each other and other platforms, including bottom nodes and gateway buoys, (c) an integrated acoustic navigation and communication network, (d) satellite sensors, and (e) a predictive model via the Regional Ocean Modeling System (ROMS) that is used to control adaptive sampling, including re-direction of satellite assets. The system composed of the above is illustrated in Fig. 1. It should be noted that the glider and mooring systems described here are but one of many variants. For example propeller-driven autonomous undersea vehicles (AUVs) transiting between bottom nodes are regarded as conceptually very similar. Here we report on our progress to date in these areas.

II. Smart Sensor Web

A. Mooring sensor system

The basic mooring system is illustrated in Fig. 1 with a block diagram in Fig. 2. The current hardware implementation was deployed and operated on the Seahurst Observatory in 40 m water depth in Puget Sound, just west of Sea-Tac International Airport. In the future it will be deployed at the MARS cabled observatory in Monterey Bay in 1,000 m water depth and at the ALOHA Cable Observatory site 100 km north of Oahu in 5,000 m water depth. Here the emphasis is on a system description [7].

The basic mooring concept is to provide the infrastructure to distribute power, communications, and precise and accurate timing throughout the water column. The mooring system consists of three main components: a near-surface float at a depth of 165 m with a secondary node and suite of sensors, an instrumented motorized moored profiler moving between the seafloor and the float that will mate with a docking station just beneath the float for battery charging, and a secondary node on the seafloor with a suite of sensors. Both secondary nodes have remotely operated vehicle (ROV)-mateable connectors available for guest instrumentation. The profiler has real-time communications with the network via an inductive modem that provides some remote control functions to allow the sampling and measurement capabilities to be focused on the scientific features of greatest interest. The power, two-way real-time communications and timing provided by cabled seafloor observatories will enable this sensor network, the adaptive sampling techniques, and the resulting enhanced science. The sampling and observational methods developed here will be transferable to ocean observatories elsewhere in the world.

Seafloor cable and EO-converters

ROV-mateable connectors on the MARS Observatory primary node will provide 375 V, 48 V, 100Base-T Ethernet, and a 1 pulse-per-second (PPS) precise timing signal (the same is available on NEPTUNE Canada, the

future NSF OOI Regional Scale Nodes, and the Aloha Cabled Observatory). The mooring system is designed for a maximum of 1200 W with 320 W for the profiler charging and 270 W for guest users. In-line electro-optical media converters (Fig. 3) are required to convert electrical communication and timing signals to optical form for transmission over any significant distance using optical fibers and back again. The seafloor and mooring riser cables both have four single mode fibers. One optical fiber is used for the Ethernet communications, and one for the PPS/RS-422 time distribution and two are spares. Wave division multiplexers (WDMs) allow bi-directional data transmission using 1310 and 1550 nm wavelengths on the fibers. The 1.5-km cable between the primary node and the seafloor secondary node junction box is a 12.7-mm diameter electrical/optical cable with six electrical conductors and the optical fibers in a 1.2-mm stainless steel tube. ROV-mateable connectors allow connection of the cable to the primary and secondary nodes. The seafloor cable (with EO converters and connectors) is installed by ROV with a reel mounted in the cable laying tool sled on the ROV; the spool will be left on the seafloor at the end of the cable laying process. In the future, EO-converters can be miniaturized and combined with the connectors at each end. When hybrid electro-optical connectors become more reliable and reasonable cost, the EO-converters could be eliminated.

Secondary nodes

The AMM has two secondary nodes that provide the same connectivity functions that are available at the primary observatory nodes, though power and communications clearly are now shared and (more) limited resources. Much of the design is based on the MARS power system (e.g., bus structure, PC-104 node controller, switching and monitoring of ports, and ground fault monitoring; see [8]).

The seafloor secondary node serves as the terminus for the seafloor EOM cable that runs from the MARS node to the base of the mooring. The node includes a frame, electronics housing, and ROV-mateable electrical connector receptacles. The mechanical design of the node was done in consultation with the ROV pilots at the Monterey Bay Aquarium Research Institute (MBARI), the operators of the MARS system. There are two guest ports in addition to ports for the seafloor cable from the primary nodes, the mooring cable (to the float node), and the instrument package. Syntactic foam buoyancy is added to make the unit just slightly negative, so the ROV can pick it up and move it around if necessary. There are receptacles for lead weights, once it is in place.

The subsurface float secondary node is connected via the mooring cable to the seafloor node next to the base of the mooring anchor. It is also connected to the AMM float instrument package and has two unused guest ports with

ROV-mateable receptacles. In addition it has the electronics for the inductive power coupler, the Sea-Bird inductive modem for communication with the profiler, an internal attitude sensor, the acoustic Doppler current profiler (ADCP), and video camera and light (looking at the profiler docking station below the float).

Science Instrument Interface Module (SIIM)

To minimize the number of ROV-wet-mateable connectors used, an intermediate multiplexer/SIIM is used to first connect all the sensors at one location together (using inexpensive dry-mate connectors); then the SIIM is connected to the secondary node housing using a single (expensive) ROV-mateable connector. This SIIM has a mix of the following features: eight ports (dry-mate connectors), power at required instrument voltages (48 Vdc or 12 Vdc), an eight-port Ethernet switch, Ethernet or RS-232 to Ethernet conversion (to connect to network), and individual software controlled load switching and deadface switching. Much of this is accomplished with a custom, easily modified, four-channel printed circuit board, a "SIIM board." Each channel has a DigiConnectME embedded module, a FET switch, and deadface relays. The DigiConnect module provides a 10/100BaseT network interface (i.e., an IP address), one high-speed RS-232 serial interface, 2 MB Flash memory, and 8 MB RAM. It provides an extremely convenient way to convert instrument RS-232 to Ethernet. It is the only "smart" device in the SIIM, and can, for instance store and forward sensor metadata. On the float and at the base of the mooring, the SIIM board is housed in a titanium pressure case rated for 5000 m. A SIIM board also resides in the float secondary node for the attitude sensor, ADCP, and Sea-Bird inductive modem. The units work well with many different oceanographic sensors connected: conductivity, temperature, depth, and oxygen ($CTDO_2$), optical backscatter, hydrophone, acoustic modem, ADCP, attitude/orientation sensor, camera/light and inductive modem. Most use RS-232 but some (e.g., the hydrophone) use Ethernet. The acoustic modem and hydrophone have access to the precise pulse-per-second timing signal.

Sensors and instruments

The Sea-Bird 52MP/43F pumped $CTDO_2$ is used throughout, two each (for redundancy) on the subsurface float and at the base of the mooring, and one on the profiler. These have titanium pressure cases rated for 6000 m. The WetLabs BBF2 sensor measures optical backscatter at 470 nm and 700 nm, and chlorophyll fluorescence within the same volume. There is one each on the float and seafloor instrument packages and on the MMP. The ADCP on the subsurface float is a RD Instruments Workhorse Quartermaster 150 kHz. It is mounted permanently on the float with a dry mate connector to the float secondary node electronics case. The ADCP has an integral attitude sensor

package. The acoustic current meter (ACM) on the profiler is a Falmouth Scientific 4-axis device measuring a 3D velocity vector. There is a broadband hydrophone (Naxys eHyd) on the subsurface float and Woods Hole Oceanographic Institution (WHOI) acoustic micromodems [9,10] on the two instrument packages; these are shown mounted on the subsurface float instrument package with SIIM in Fig. 4.

A gyro enhanced orientation sensor in the float secondary node is installed to better understand the float/mooring dynamics, related stresses, and impact on the optical fibers; it will help answer the question, is a swivel necessary in future mooring systems like this? If no swivel is needed, a major engineering simplification in the mooring can be made. There is a color video camera with lights mounted below the subsurface float looking at the profiler dock to monitor the MMP docking and undocking.

Moored profiler

The McLane Moored Profiler (MMP, [11]) has been modified for this application. The changes include: new motor, gearbox, and wheel for use with the larger EOM cable; interface for Wet Labs and Seabird sensors; interface APL-UW moored profiler controller (MPC) to the MMP controller to offload data after every profile; replace primary Li battery pack with rechargeable 860 W h Li-ion battery bank mounted in glass sphere; mount for inductive charging coupler and electronics; and use extended length McLane housing with additional glass sphere for rechargeable battery bank and for increased buoyancy. With these changes, there is a data collecting-to-battery charging duty cycle of 95% (4 days operation with 4 h charging). The MPC (a Persistor CF-2 processor) collects the BB2F optical data (backscatter and fluorescence), interfaces with and downloads data from the MMP ($CTDO_2$, ACM, engineering data), interfaces with and transfers data/commands to/from the shore server, and supervises the charging of the battery pack.

The appropriate MMP software to enable adaptive sampling has only recently become available ("patterns" and schedule file transfers at the end of any profile). In the future the profiler will be modified to be ROV serviceable. By this we mean an ROV can remove and install it without disturbing the deployed mooring. There are three reasons for this: (1) reliability of the MMP is not yet as good as desired, (2) any profiler is a mechanical device prone to failure, and (3) irrespective of profiler reliability, one may want to or need to change out the profiler with its load of sensors, either because of sensor calibration/biofouling, or for a different payload. With this capability, the basic mooring system, with expected long life, can remain in place.

Inductive Power System (IPS)

The inductive power system (IPS) to charge the batteries on the profiler is a key new technical development of the project. The McLane Mooring Profiler (MMP) will periodically connect or "dock" beneath the mooring float to charge its battery pack. Due to the fact that the system is submerged in conducting seawater, the connection must not utilize any contacts that allow an electrical connection to contact the seawater. Wet-mateable connectors that have enclosed, oil-bathed contacts have some potential for this but they typically require a relatively high mating force and have a limited number of mate/de-mate cycles. The technique that has been selected is to use inductive coupling for the power. S&K Engineering has a significant amount of experience in the electric automobile industry and was contracted to make the inductive power coupler (the "dock") and the associated drive and charging electronics.

A block diagram of the charging system is shown in Fig. 5. The float side has a high voltage dc-power source that can range from 150 to 400Vdc. A boost DC-DC converter is used to create a pre-regulated voltage at 375Vdc for the second stage. The main power transfer through the inductive coupler is driven by a half-bridge inverter driving a series resonant tank circuit. The inverter operates at a constant switching frequency of 50 kHz that is above the resonant frequency. The inductive coupler has a primary side that is fixed to the mooring cable and a secondary side that is mounted on the profiler. Because of the need to operate for an extended period of time in the presence of bio-fouling, the coupler has been designed with an annular gap of 2 mm. Because of this relatively large gap, the coupler has a much larger cross-sectional area than a typical power transformer. The coupler has 10 turns on the primary and 3 turns on the secondary. Because of the relatively large gap (2 mm) and the separation of the windings, the coupler functions as a poorly coupled transformer and produces significantly less voltage or current in the secondary than an ideal transformer. The seawater also appears as a moderate impedance load that reduces the power conversion efficiency. The secondary side has a full-wave rectifier that may be shunted by a FET switch. The system is designed to deliver 250W at 16.4Vdc on the secondary side, with an efficiency > 70 per cent. Fig. 6 shows the system components, Fig. 7 shows the profiler being deployed in Puget Sound and in the docking position on the mooring. The charging cycle is shown in Fig. 8; about two-thirds of the charge is accomplished in 2 hours and a full charge of the batteries (849 W-h Lithium Ion) takes 5 hours. Future versions will have a more robust ferrite construction, as the current one chipped in places. The coupling mechanism will be reversed so the spring-loaded portion is hanging down on the mooring wire. More detail can be found in [12].

Inductive Modem (IM) communications

The Sea-Bird Inductive Modem (IM) system is used for communications between the float and the MMP. Communications rate is nominally 150 bytes/s; with forward error correction and other overhead the effective rate is 90 bytes/s. This slow link is a bottleneck and will be replaced with a newer 19.2 kbaud system that can also provide ~30 μs timing accuracy.

Mooring riser cable

The 22-mm (0.85-inch) diameter mooring cable has six 18 AWG conductors with polypropylene insulation, four loose fibers in a 1.3-mm diameter steel tube (in center), a Kevlar strength member, and a steel mesh for fish bite protection, all enclosed in a polyurethane jacket. This cable, connecting the seafloor secondary node to the subsurface float and the float secondary node, has electrical connector terminations and EO converters identical to the seafloor cable connecting the MARS primary node to the seafloor secondary node. Initial pull tests of the cable with the mechanical terminations failed; the terminations were improved and the tests were completed successfully.

Mooring float

The subsurface float tensions the mooring riser cable and serves as an instrument platform. Fig. 9 shows the float and structure with the float instrument package and ADCP. The 300-m depth rated syntactic foam float is 1.8 m diameter, 0.8 m high, weighs 2052 lbs in air, and has a buoyancy of 2375 lbs. The float structure is made from 6061-T6 painted aluminum. An electro-mechanical swivel/slip ring assembly is used at the top end of the mooring cable just beneath the subsurface float. The swivel has 16 slip rings in an oil-filled, pressure-compensated housing with an external pressure compensator (visible in the top of the lower panel of Fig. 7). The stainless steel swivel is rated at three metric tonnes (6600 lbs) working load.

Software

The successful operation of the mooring sensor network depends on software. The mooring system uses a scaled-down version of the MARS power monitoring and control system (PMACS; [8]) with the secondary node controller (SNC) serving a similar role as the MARS node power controller. The SNC (a PC-104 stack) monitors load current and bus voltage, allows for the setting of per-load current limits, and provides circuit-breaker and ground-fault monitoring capabilities. The PMACS server communicates with the SNC via an XML-RPC interface. The shore server (SS) runs a dedicated process for each sensor (an instrument server process). Each process interfaces to its respective sensor over the network and archives the sensor data on the local disk. All sensor configuration tasks are handled through the SS. In total, there are 36 IP addresses required.

The profiler has required a significant amount of software associated with the transfer of data from the MMP controller, communications over the inductive modem, acquisition of data from non-MMP sensors (the BB2F), and the battery charging/docking process.

Testing in Puget Sound

The mooring system was tested in Puget Sound on several occasions between June 2007 and August 2008 with success. An example of a temperature time series from the profiler is shown in Fig 10. The profiler was programmed to transit vertically every 15 minutes. An example of hydrophone data is shown in Fig. 11. The hydrophone bandwidth is from 5 Hz to 30 kHz. At the Seahurst Observatory (a high school marine center) the sampling was limited to 12 kHz because of storage and communications bandwidth limitations between the shore station and APL. This figure shows a representative spectrogram with both acoustic modem activity (the two thick bands) and the ADCP going off every second.

B. Seaglider

The basic Seaglider developed at the University of Washington's Applied Physics Laboratory (UW/APL) can dive to 1000 m while moving horizontally at about ½ knot using ½ W of power. Glider missions have now exceeded 737 dives, covering 4,900 km over ground and 279 days. Gilders routinely collect temperature and conductivity (salinity) data during a dive. We have adapted the Seaglider to carry a broadband hydrophone (10 Hz – 30 kHz) and a WHOI acoustic micromodem [9]; see Figs. 12 and 13. The latter operates in the 23 – 27 kHz band.

C. Acoustic communications and Network Infrastructure

There is currently much activity within the oceanographic community to develop integrated underwater sensor networks that include mobile, fixed, autonomous, and cabled nodes. A significant difficulty in this effort is that the the underwater ocean environment, especially in shallow water, is in general a very challenging medium in which to reliably communicate information. The reasons are well documented [13,14]. Since radio frequency (RF) waves attenuate extremely rapidly underwater, acoustic signaling is the preferred method of underwater wireless communication. Low acoustic sound speed (1,500 m/s) introduces long propagation delays and extensive time spreading of the received signal. The shallow ocean environment is a dense scattering environment and is generally highly time varying. Acoustic signals attenuate very quickly as frequency increases; hence, the underwater channel is bandwidth limited. Furthermore, underwater Seagliders, such as those used in this project, are low power battery operated devices. This imposes practical constraints on the complexity of communications hardware [15,16].

Testing has taken place of acoustic communications between gliders and between gliders other platforms, both fixed and mobile, at the surface, in the water column, and on the bottom. In one such test in Puget Sound, a glider sat on the bottom and communicated with a glider moving out in range; see Fig. 14. Travel time and thus range was routinely measured. Frequency shift-key (FSK) signal coding at 80 bits per second (b/s) was used, with reliable results to 4 km and less reliable results to 7 km. In another test, an acoustic modem was installed on the AMM bottom node at 30 m water depth as part of the mooring testing at the Seahurst Observatory in Puget Sound (just west of Sea-Tac airport). Using a boat deployed transducer and deck box, ranges to 2.5 km were obtained (see Fig. 15); the lower ranges than in the first mentioned test were likely a result of the much shallower bottom. In more recent testing, phase-shift-key (PSK) signal coding (coherent vs. the incoherent FSK) was used. In this case 240 b/s and 5200 b/s were obtained between a glider and a surface gateway buoy with a modem suspended beneath; this modem has a 4-element hydrophone-receiving array. Further, a go-to-surface command was sent to the glider to demonstrate real-time vehicle control via the acoustic communications channel. In all cases, one-way travel times were obtained from which range is obtained. In summary, these test results confirm that the acoustic modem can perform adequately both from a communications perspective as well as for navigation. This demonstrates a necessary capability for the NSF OOI, to communicate between fixed and moving infrastructure.

In related work, the acoustic recording system on the glider was used to collect marine mammal data during an experiment in Monterey Bay in 2006. Many blue, fin, humpback, and sperm whale calls were detected, as well as birds and sea lions [17]. In another mission off the Hawaiian Island of Kauai, the glider recorded transmissions from a 75 Hz bottom mounted acoustic source (part of the Acoustic Thermometry of Ocean Climate / North Pacific Acoustic Laboratory project [18,19]). Coherent signal processing with near-theoretical gain was achieved with positive ray identification. This indicates that gliders can coherently average these low frequency signals over 10 minutes, and estimate Doppler velocity very accurately. Thus, they can serve as mobile tomography receivers. These results are examples of using basic acoustics infrastructure for navigation and communication, as well as science and other uses. Further, the Kauai results indicate that the same low frequency sources can serve as underwater “GPS” transmitters for basin scale navigation and communication.

D. Satellite Sensors

Of most direct relevance for determining the physical state of the ocean from space are sensors that determine sea surface height and wind stress. Sea surface height is measured with an altimeter, e.g., Jason-2, and provides a

measure of depth integrated density; from this can be inferred heat content and upper ocean currents via geosptrophy. Wind stress is estimated from wind speed as determined by a scatterometer, e.g., SeaWinds on the QuikSCAT satellite, which infers wind speed from surface roughness. The SeaWinds scatterometer is a specialized microwave radar that measures near-surface wind velocity (both speed and direction) under all weather and cloud conditions over Earth's oceans. SeaWinds collects data in a continuous 1,800-kilometer-wide band, making approximately 400,000 measurements and covering 90% of Earth's surface in one day. Further, satellite measurements of sea surface temperature provide additional observations.

In the future, a wide-area swath altimeter system (Surface Water and Ocean Topography, SWOT) will provide orders of magnitude more data on the ocean surface topography. In other missions, the estimation of wind speed will be improved with the Extended Ocean vector Winds Mission (XOVWM) and surface salinity (affecting ocean density among other things) will be measured by the Aquarius mission [20]. These and many other space-based sensors will be used in smart sensor webs as they develop over time.

E. Regional Ocean Modeling System (ROMS)

Despite the recent advance of the ocean observing technology, sampling the ocean on both the global and regional scales remains a challenging task. While satellite sensors can only measure the surface properties of the ocean (including the surface manifestations of subsurface processes, such as with altimetry) with imperfect, though improving, time-space global sampling, there are usually large temporal and spatial gaps between in situ sensors. Three-dimensional dynamical models are therefore needed to combine these in situ and satellite measurements in a process known as data assimilation. The goal is to estimate the state of the ocean today and then to predict its future evolutions.

We are using the Regional Ocean Modeling System (ROMS), a community based and openly available software (http://www.myroms.org). ROMS solves the three-dimensional oceanic equations of momentum, temperature and salinity [21]. The model uses a vertical coordinate following the bottom topography [22]. Compared with the traditional sigma-coordinate system, this vertical coordinate system provides more flexibility in choosing vertical levels in specific vertical domains, such as the bottom boundary layer or surface mixed layer. The model explicitly represents the time evolution of the free-surface and has an open lateral boundary condition to allow the exchange of information through boundaries [23]. The Flather boundary condition [24] is used to allow the propagation of barotropic tidal signals into the domain.

The ROMS configuration used here includes a fully resolved tidal component. ROMS uses data from the Topex-Poseiden Global Inverse Solution version 6.0 (TPXO.6) developed at the Oregon State University [25]. The tides are provided as complex amplitudes of earth-relative sea-surface elevation and tidal currents for eight primary harmonic constituents (M2, S2, N2, K2, K1, O1, P1, Q1), on a 1/4 degree resolution grid. These harmonics are introduced in ROMS through the open boundaries using the Flather condition (see [23]). This open boundary condition combines the Sommerfeld equation (with surface gravity wave phase speed) with a 1-D version of the continuity equation applied in the outwardly normal direction at each open boundary. The volume is automatically conserved in the domain and variations due to physical forcing such as tides (but also the other subtidal components) are introduced through the external data. Preliminary results from the ROMS solutions with tidal forcing show that the coastal ocean is dominated by the semi-diurnal (M2) tide with an error less than 5% for both amplitude and phase [26].

ROMS can be implemented in a multi-nested grid configuration that allows for telescoping from the large-scale down to regional and local region at very high resolution (on the order of 1 km). Fig. 16 shows a 3-domain nested ROMS configuration centered around Monterey Bay, California. The spatial resolutions are 15-km, 5-km, and 1.5-km, respectively. The Monterey Bay ROMS configuration has been tested in two major field experiments: Adaptive Sampling Ocean Network (AOSN) in 2003 [27], Adaptive Sampling and Prediction (ASAP) in 2006.

ROMS has the ability to assimilate both in situ and satellite data using a 3-dimensional variational data assimilation (3DVAR) method [28,29]. During both field experiments, the ROMS modeling and data assimilation system was run daily in real-time, assimilating satellite data as well as in-situ temperature and salinity vertical profile data (e.g., derived from CTD measurements on moorings, ships, gliders, and autonomous underwater vehicles or AUVs). The current ROMS configuration produces nowcasts every six hours. Forced with the mesoscale atmospheric forecast [30], the current ROMS configuration makes a 48-hour forecast every 24 hours. Initial results show significant skill in the ROMS model in describing and predicting the coastal circulation and variability [31].

During the 2006 ASAP field experiment, we have demonstrated the significant positive effect of adaptive sampling using gliders to improve the model simulation and forecast [32]. This effectiveness may be maximized if the observations are "targeted" based on objective guidance that is derived from models (Fig. 17). Such guidance can answer the question: "What are the optimal sampling locations in the next two days, in order to reduce the errors in the ROMS forecast within a region of interest?" Fig. 17 shows an example of the guidance showing the

uncertainty and dynamics of the flow that can be derived from the ROMS ensembles. Formally, the guidance represents the reduction in prediction error variance within a given region. Based on this guidance, we have identified optimal locations for additional sampling. One additional glider was deployed to collect more data around these optimal locations. Fig. 18 shows the RMS differences in temperature and salinity between all glider measurements within the observational box and the co-located ROMS reanalysis values. Two curves are shown, one for the ROMS reanalysis that does not assimilate this additional glider data and another for the reanalysis that does assimilate this glider data. The reanalysis that includes this adaptively deployed glider data shows a significant improvement (i.e., smaller RMS errors), at least in part, due to the adaptive sampling.

During 13-23 October 2008, another field experiment was conducted in Monterey Bay (MB08). The major science goal was to detect and predict extreme blooms in Monterey Bay using a smart sensor web-integrating in situ and remote sensing observations with predictive models. A unique innovation of MB08 was to bring the adaptive sampling concept to the satellite platform, for the first time. The objective was to demonstrate the ability to detect and predict extreme blooms using an observatory concept consisting of both in situ and remote sensing platforms as well as real-time ocean and atmospheric forecasting models.

Recent efforts have included feasibility pilot tests to track oceanographic events using sensor web technologies. Wide coverage satellite assets such as MODIS and MERIS have ocean color products useful in studying algal blooms. However these wide coverage sensors have lower spatial resolution. Ideally these datasets would be combined with point-and-shoot satellite data with less spatial coverage but higher spatial (and possibly spectral) resolution.

During MB08, the Earth Observing 1 (EO-1) satellite was tasked to automatically deliver oceanographic science data products for scientist evaluation. The EO-1 Hyperion high-resolution hyperspectral imager is capable of resolving 220 spectral bands (from 0.4 to 2.5 μm) with a 30-meter resolution. The instrument can image a 7.5 km by 100 km area per image, and provide detailed spectral mapping across all 220 channels with high radiometric accuracy. Specifically in this case, EO-1 Hyperion acquisitions were made in coordination with the EO-1 Sensorweb team on 10 days in September and October 2008 with 5 scenes during the MB08 deployment. EO-1 used automated workflows to process and deliver the data to the MB08 science and operations team along with two derivative science products, Fluorescence Line Height (FLH) and Maximum Chlorophyll Index (MCI) linear baseline data products. These automated sensor web workflows were triggered by the campaign tag associated with the acquired

scenes and invoked perl/IDL processing to produce the desired science products. The resultant science products were automatically delivered to the scientists through a collaboration web portal. The system posted web updated the portal with links to files downloadable from EO-1 servers. This capability was later generalized to enable sftp and email delivery of products as well. These efforts demonstrated the utility of automated science processing and delivery of EO-1 products to support science operations and also provided guidance on areas of improvement needed before operationally useful products could be delivered. Key operational areas identified for future work include improved instrument and atmospheric correction.

The ultimate goal is to eventually develop automated processing flows that deliver alerts and science classification products to interested scientists and authorities. These automated alerts could then be used to deliver data to interested authorities and also request subsequent data to track the evolving phenomena.

III. Discussion

The foregoing presentation of sensor web elements and results is part of an ongoing, evolving effort to improve the ocean observing system. The current generation of satellite and in situ observations are a great improvement over a decade ago, but they are inadequate for future needs. Improvements in satellite sampling have been called for as part of the NASA "Decadal Plan," for example (the SWOT and XOVWM mentioned above were examples of planned missions, [20]), and some of these are being funded. These missions will better sample the ocean surface in space and time but there are fundamental limits to how deep into the ocean this boundary condition information can propagate, given the uncertainties in our knowledge of the physics and the uncertainties of the measurements. In situ measurements will always be required to keep models on track. In the international Ocean Observations 2009 conference [2], there was a call to improve the present system with elements such as glider fleets and tomographic sampling of the deep ocean and under ice-covered water (e.g., the Arctic Ocean and off Antarctica) [33, 34].

Quantification of the overall efficacy of any particular ocean measurement or measurement type with associated instrument platform is a on-going effort within the ocean modeling and data assimilation community. It is only now that the models and data assimilation tools have the fidelity and sophistication to capture the important information content of a data type. Simulation and actual experiments to determine the efficacy of the mooring plus glider combination have not been conducted. It is known, though, that glider data is significant in this regard, because, even though slow, a glider can move several times faster than typical ocean advection speeds and thus can capture some of the dynamics. In general, a fixed-point measurement by itself is less effective because of the high levels of

high frequency and high wavenumber "noise" (e.g., internal waves) relative to the ocean mesoscale that is typically the main signal of interest in ocean observing. However, the fixed individual platforms typically can collect data that are of more interest for process studies or long-term climate studies. Further, when fixed platforms are in an array configuration, such as the TAO-TRITON array across the equatorial Paciific, they too can synoptically capture the large-scale features of interest.

We see the primary use of acoustic communications in ocean sensor webs being the transfer of data and commands between fixed and mobile subsea platforms and the surface to shore and back. Because the air-sea interface is so inhospitable, the number of gateways through the interface will always be limited. Rather, much of the sensor web will remain below the surface in more hospitable domains and rely on specialized platforms to provided the gateway capability. Further, through the transfer of data between elements of the web, the sampling can be made more efficient, either using truly autonomous in situ decision making, or by relying on more centralized command and control.

Sensor web elements such as we have described here can contribute to these future efforts, evolving with time. For instance, the same cabled mooring systems can host acoustic transceivers, serving the role of "underwater GPS satellites" for long(er) range navigation as well as communications. While providing the more conventional temperature and salinity point profile data, seagliders (or other fixed or mobile platforms) can serve as acoustic tomography receivers providing complementary data. As an integrated web, instruments and platforms can serve multiple purposes.

A sensor web as envisioned and developed here complements existing and planned space science missions. Specifically the sensor web integrates space-based sensor data with in-situ data; these are integrated via the ROMS model, the output of which can used for achieving a set of scientific objectives, including enhancing the science products of stand-alone missions such as described for the MB08 example. The ROMS model is also useful in planning future space-based missions and in situ observing programs dedicated to climate change science.

IV. Concluding Remarks

The ocean-observing smart sensor web presented herein is composed of (a) a cable-connected mooring system with a profiler under real-time control with inductive battery charging; (b) a glider with integrated acoustic communications and broadband receiving capability; (c) satellite sensor elements; (d) an integrated acoustic navigation and communication network; and (e) a predictive model via the Regional Ocean Modeling System

(ROMS). The acoustic communications network forms a critical link in the web between the in-situ sensors and shore control, and thus space-based sensors, and facilitates adaptive sampling and calibration. As an example of the power of the sensor web concept, during MB08 we were able to adjust the looking angle of the Hyperion sensor on board the EO-1 satellite as it passed over Monterey Bay. This is the first time that satellite measurements were guided by in situ observations and model simulations and forecasts in real time without manual intervention, therefore closing a complete loop of a smart sensor web from ocean observing to model forecast leading to future guided observations.

ACKNOWLEDGMENTS

This work reported here has been funded in large part by three projects. The integrated underwater/satellite sensor network science and technology development is funded by the NASA Earth Science Technology Office's Advanced Information Systems Technology (AIST) Program under award number AIST-05-0030. The mooring work was funded by the National Science Foundation (NSF) Ocean Technology and Interdisciplinary Coordination (OTIC) program, Grant OCE 0330082. The acoustic Seaglider work was funded by the Office of Naval Research (ONR), Grant N00014-05-1-0907. Part of the research described in this paper was carried out, in part, at the Jet Propulsion Laboratory (JPL), California Institute of Technology, under contract with the National Aeronautics and Space Administration (NASA). Computing support from the JPL Supercomputing Project is acknowledged.

Thanks are given to the many scientists, engineers, technicians and students who have contributed to this work.

REFERENCES

[1] Wunsch, C., R. Ponte and P. Heimbach, "Decadal trends in sea level patterns", *J. Clim.* vol. 2024, pp. 5889–5911, 2007.

[2] Hall, J., D. E. Harrison, and D. Stammer, Eds. *Proceedings of OceanObs'09: Sustained Ocean Observations and Information for Society*, Venice, Italy, 21-25 September 2009, ESA Publication WPP-306, in press, 2010.

[3] Cazenave, A., D. P. Chambers, P. Cipollini, L. L. Fu, J. W. Hurell, M. Merrifield, R. S. Nerem, H. P. Plag, C. K. Shum, and J. Willis, Sea level rise: regional and global trends, Plenary Paper In *Proceedings of OceanObs'09: Sustained Ocean Observations and Information for Society (Vol. 1)*, Venice, Italy, 21-25 September 2009, Hall, J., Harrison, D.E. & Stammer, D., Eds., ESA Publication WPP-306, in press, 2009.

[4] B. M. Howe, T. McGinnis, and M.L. Boyd, Sensor Network Infrastructure: Moorings, Mobile Platforms, and Integrated Acoustics, S*ymposium on Underwater Technology 2007 and Workshop on Scientific Use of Submarine Cables & Related Technologies 2007*, University of Tokyo, 17-20 April 2007.

[5] B.M. Howe, P, Arabshahi, W. L. J. Fox, S. Roy, T. McGinnis, M. L. Boyd, A. Gray, and Yi Chao, "A smart sensor web for ocean observation: system design, architecture, and performance," *Proc. 2007 NASA Science Technology Conference*, University of Maryland, June 19-21, 2007.

[6] Howe, B. M., N. Parrish, L. Tracy, A. Gray, Y. Chao, T. McGinnis, P. Arabshahi, and S. Roy, A Smart Sensor Web for Ocean Observation: Integrated Acoustics, Satellite Networking, and Predictive Modeling, *2008 NASA Science Technology Conference (NSTC2008)*, University of Maryland, 24-26 June 2008.

[7] Howe, B. M., T. McGinnis, J. Gobat, Moorings for Ocean Observatories: Continuous and Adaptive Sampling, *Proceedings, the Scientific Submarine Cable 2006 Conference*, 172-181, Marine Institute, Dublin Castle, Dublin, Ireland, 7-10 February 2006.

[8] Howe, B. M., T. Chan, M. El-Sharkawi, M. Kenney, S. Kolve, C.C. Liu, S. Lu, T. McGinnis, K. Schneider, and C. Siani, H. Kirkham, V. Vorperian, P. Lancaster, Power System for the MARS Ocean Cabled Observatory, *Proceedings, the Scientific Submarine Cable 2006 Conference*, 121-126, Marine Institute, Dublin Castle, Dublin, Ireland, 7-10 February 2006.

[9] Freitag, L., M. Grund, S. Singh, J. Partan, P. Koski, and K. Ball, The WHOI micro-modem: An acoustic communications and navigation system for multiple platforms, *Proceedings of the MTS/IEEE Oceans Conference*. 2005.

[10] Freitag, L., M. Stojanovic, M. Grund, S. Singh, Acoustic Communications for Regional Undersea Observatories, *Proc. Oceanology International 2002*, London, March 2002.

[11] Alford, M. H., M. C. Gregg, and M. A. Merrifield, 2006. Structure, propagation, and mixing of energetic baroclinic tides in Mamala Bay, Oahu, Hawaii. J. Phys. Oceanogr., 36, 997-1018.

[12] McGinnis, T., C. P. Henze, and K. Conroy, Inductive Power System for Autonomous Underwater Vehicles," Oceans 2007, 1-5, 29 September 2007 - 4 October 2007.

[13] Stojanovic, M., Recent advances in high-speed underwater acoustic communication, *IEEE J. Oceanic Eng*., vol. 21, pp 125-136, 1996.

[14] Kilfoyle, D. B., and A.B. Baggeroer, The state of the art in underwater acoustic telemetry, *IEEE J. Oceanic*

Eng., vol. 25, pp 4-27, 2000.

[15] Roy, S., P. Arabshahi, D. Rouseff and W. Fox, Wide area ocean networks: architecture and system design considerations, *Proc. 1st ACM International workshop on Underwater networks*, 2006.

[16] Parrish, N., L. Tracy, S. Roy, W.L.J. Fox, and P. Arabshahi, System design considerations for undersea networks: link and multiple access protocols, IEEE Journal on Selected Areas in Communications, vol. 26, no. 9, December 2008.

[17] Moore, S. E., B. M. Howe, K. M. Stafford, and M. L. Boyd, Including whale call detection in standard ocean measurements: applications of acoustic Seagliders, J. Marine Technology Society, 41, 53-57, 2008.

[18] ATOC Instrumentation Group: B. M. Howe, S. G. Anderson, A. Baggeroer, J. A. Colosi, K.R. Hardy, D. Horwitt, F. Karig, S. Leach, J. A. Mercer, K. Metzger, Jr., L. O. Olson, D. A. Peckham, D. A. Reddaway, R. R. Ryan, R. P. Stein, K. von der Heydt, J. D. Watson, S. L. Weslander, and P. F. Worcester, Instrumentation for the Acoustic Thermometry of Ocean Climate (ATOC) prototype Pacific Ocean array, Proc. Oceans '95 MTS/IEEE, San Diego, California, 1483–1500, 1995.

[19] Dushaw, B. D., P. F. Worcester, W. H. Munk, R. C. Spindel, J. A. Mercer, B. M. Howe, K. Metzger, Jr., T. G. Birdsall, R. K. Andrew, M. A. Dzieciuch, B. D. Cornuelle, and D. Menemenlis, A decade of acoustic thermometry in the North Pacific Ocean, J. Geophys. Res., 114, C07021, doi:10.1029/2008JC005124, 2009.

[20] National Research Council (NRC), Earth Science and Applications from Space: National Imperatives for the Next Decade and Beyond, National Academies Press, 2007.

[21] Shchepetkin, A.F., and J.C. McWilliams, 2004: The Regional Oceanic Modeling System: A split-explicit, free-surface, topography-following-coordinate ocean model. Ocean Modelling 9, 347-404.

[22] Song, Y. T. and D. Haidvogel, 1994. A semi-implicit ocean circulation model using a generalized topography-following coordinate system, *J. Comput. Phys*., Vol. 115, 228-244.

[23] Marchesiello, P., J. C. McWilliams, and A. Shchepetkin, Open boundary condition for long-term integration of regional oceanic models, *Ocean Modelling*, Vol. 3, 1-21, 2001.

[24] Flather, R. A., A tidal model of the north-west European continental shelf, Mem. Soc. Roy. Sci. Liege, Vol. 6, 141-164, 1976.

[25] Egbert, G. D., A. F. Bennett, and M. G. G. Foreman, TOPEX/POSEIDON tides estimated using a global inverse model, *J. Geophys. Res*., Vol. 99, 24821-24852, 1994.

[26] Wang, X., Y. Chao, C. Dong, J. Farrara, Z. Li, J.C. McWilliams, J. D. Paduan, L. K. Rosenfeld, Modeling tides in Monterey Bay, California, Journal title: Deep-Sea Research Part II, Reference: DSRII2394, 2009.

[27] Ramp, S.R, P. Lermusiaux, R. E. Davis, Y. Chao, D. Fratantoni, N.E. Leonard, J.D. Paduan, F. Chavez, I. Shulman, J. Marsden, W. Leslie, and Z. Li: Preparing to predict: The Second Autonomous Ocean Sampling Network (AOSN-II) experiment in the Monterey Bay, *Deep Sea Research II,* 56, 68-86, doi:10.1016/j.dsr2.2008.08.013, 2009.

[28] Li, Z., Y. Chao, J. C. McWilliams, and K. Ide (2008): A three-dimensional variational data assimilation scheme for the Regional Ocean Modeling System: Implementation and basic experiments. J. Geophys. Res., 113, C05002, doi:10.1029/2006JC004042, 2008.

[29] Li, Z., Y. Chao, J.C. McWilliams, and K. Ide: A Three-Dimensional Variational Data Assimilation Scheme for the Regional Ocean Modeling System. *Journal of Atmospheric and Oceanic Technology*, 25, 2074-2090, 2009.

[30] Doyle, J. D., Q. Jiang, Y. Chao, J. Farrara: High-resolution real-time modeling of the marine atmospheric boundary layer in support of the AOSNII field campaign. *Deep-Sea Research II*, 56, 87-99, doi:10.1016/j.dsr2.2008.08.009, 2009.

[31] Chao, Y., Z. Li, J. Farrara, J. C. McWilliams, J. Bellingham, X. Capet, F. Chavez, J.-K. Choi, R. Davis, J. Doyle, D. Frantaoni, P. P. Li, P. Marchesiello, M. A. Moline, J. Paduan, S. Ramp: Development, implementation and evaluation of a data-assimilative ocean forecasting system off the central California coast. Deep-Sea Research II, doi:10.1016/j.dsr2.2008.08.011, 2009.

[32] Chao, Y., Z. Li, J. Farrara, J. C. McWilliams, J. Bellingham, X. Capet, F. Chavez, J.-K. Choi, R. Davis, J. Doyle, D. Frantaoni, P. P. Li, P. Marchesiello, M. A. Moline, J. Paduan, S. Ramp: Development, implementation and evaluation of a data-assimilative ocean forecasting system off the central California coast. Deep-Sea Research II, doi:10.1016/j.dsr2.2008.08.011, 2009.

[33] Dushaw, B., et al., A global ocean acoustic observing network, Community White Paper in Proceedings of OceanObs'09: Sustained Ocean Observations and Information for Society (Vol. 2), Venice, Italy, 21-25 September 2009, Hall, J., Harrison, D.E. & Stammer, D., Eds., ESA Publication WPP-306, in press, 2010.

[34] Howe, B. M., and J.H. Miller, "Acoustic sensing for ocean research," J. Mar. Tech. Soc., 38, 144–154, 2004.

List of Figure Captions

Fig. 1. The ALOHA-MARS mooring system, using acoustic Seagliders and satellite data to extend the spatial sampling footprint.

Fig. 2. Mooring system block diagram.

Fig. 3. ROV-mateable connectors and the electro-optical converters (in beryllium copper pressure cases) attached to each end of the (black) seafloor cable.

Fig. 4. (top) Detail of the hydrophone (small black cylinder inside the clear tube) and the WHOI micromodem transducer (larger black cylinder). (bottom) The complete instrument package on the deck of the R/V *Thompson* prior to deployment at the Seahurst Observatory; the micromodem electronics is strapped in the corner. The SIIM pressure case is visible with a yellow APL sticker. The CTDs and BB2F are behind the SIIM. The white block is syntactic foam to make the package near neutral buoyancy. The float secondary node is the Delrin cylinder to the right (all the connectors are on the hidden end).

Fig. 5. Inductive Power System Block Diagram. A series resonant converter drives a constant frequency square wave voltage across the inductive coupler that is rectified and regulated on the secondary side.

Fig 6. The inductive power system (IPS) components.

Fig. 7. (top) Deploying the MMP. The inductive power system primary is at the very top on the mooring cable, the secondary is on top of the profiler. The acoustic current meter has the 4 arms in the middle. The CTD sensors are wrapped in anti-fouling copper tape. (lower) The MMP on the mooring in Puget Sound in the docking position. One electro-optical converter is above the dock followed by a D-plate and the electro-mechanical swivel.

Fig. 8. Plot of the battery voltage and current during charging, measured at the battery.

Fig. 9. The subsurface float. The instrument module with two CTDs is on the left; TM is plugging in the ROV mateable connector, connected to the secondary node in the left background. The ADCP it top right. A titanium post fits into the slot in the float.

Fig 10. Temperature as a function of depth (vertical axis) and time (horizontal axis). Warm (and salty) bottom intrusions associated with tidal flow are clear.

Fig. 11. Hydrophone spectrogram showing two strong modem signals (saturated, aliased here) and the ADCP transmissions at 1 second intervals.

Fig. 12. The acoustic Seaglider. The hydrophone is in tail cone at the top, the acoustic modem transducer beneath it. The body contains (left to right) an acoustic emergency locator transponder/altimeter, electronics and low voltage batteries, high voltage batteries on a mass shifter for changing pitch and roll, buoyancy engine (oil pump) with internal and external oil bladder, and GPS and Iridium antenna.

Fig. 13. Acoustic Seaglider being recovered after a Monterey Bay mission (courtesy J. Curcio).

Fig. 14. Signal quality versus range and depth. Signal quality ranges from 253 (high signal-to-noise ratio) to 100 (low SNR). One glider is sitting on the bottom communicating with another glider making multiple dives. Data from Puget Sound tests conducted summer 2007.

Fig. 15. Acoustic modem results from Seahurst tests: (top) signal quality versus time, (middle) travel time versus time, (bottom) quality versus range.

Fig. 16. Sea surface temperature as simulated by the three nested ROMS models with a spatial resolution of 15-km (left), 5-km (middle), and 1.5-km (right), respectively.

Fig. 17. ROMS-derived guidance aimed at improving a 1-day ROMS prediction within the blue rectangle region. Darker shading corresponds to preferred locations for sampling targeted observations of (A) temperature and (B) salinity.

Fig. 18. ROMS reanalysis RMS errors in (A) temperature and (B) salinity before (solid line) and after (dashed line) the adaptive sampling deploying a glider following the ROMS derived guidance.

Figures

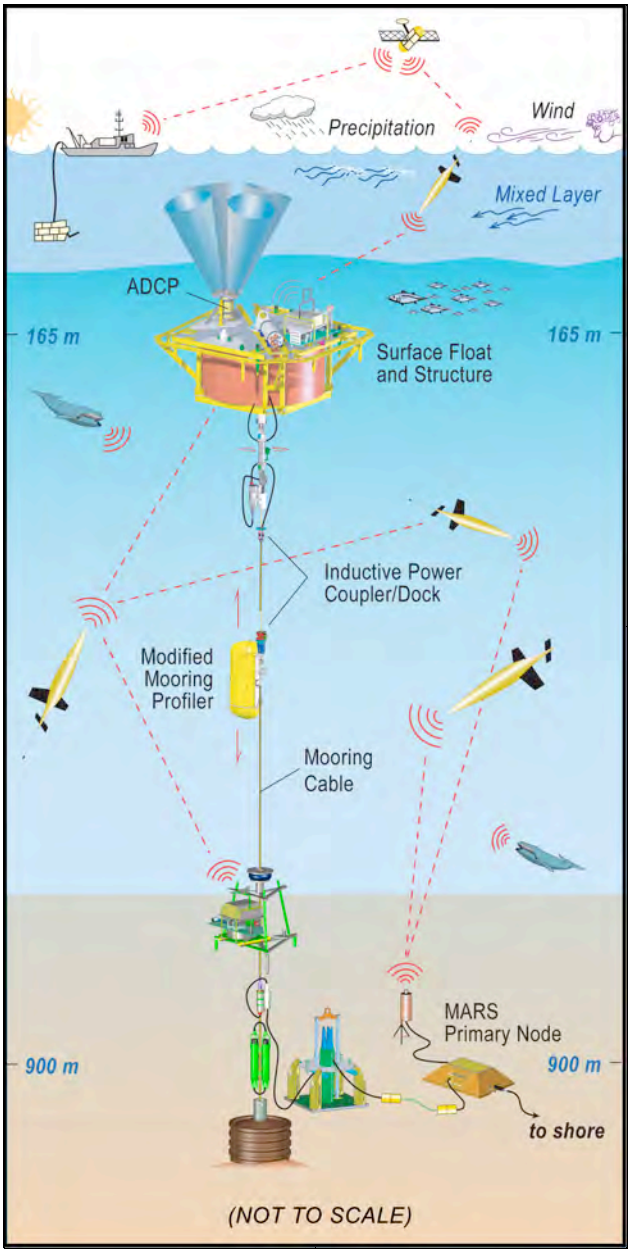

Fig. 1. The ALOHA-MARS mooring system, using acoustic Seagliders and satellite data to extend the spatial sampling footprint.

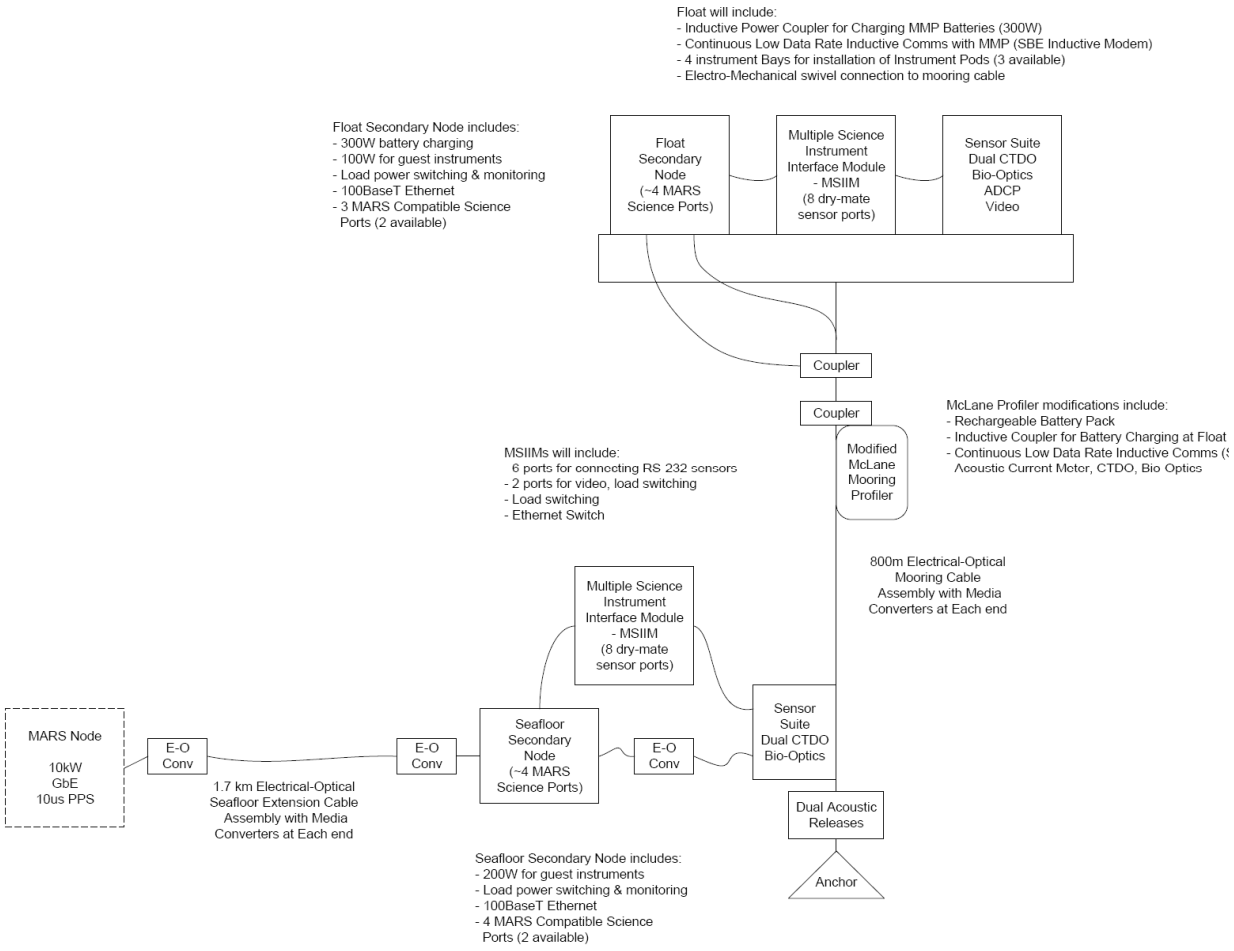

Fig. 2. Mooring system block diagram.

Fig. 3. ROV-mateable connectors and the electro-optical converters (in beryllium copper pressure cases) attached to each end of the (black) seafloor cable.

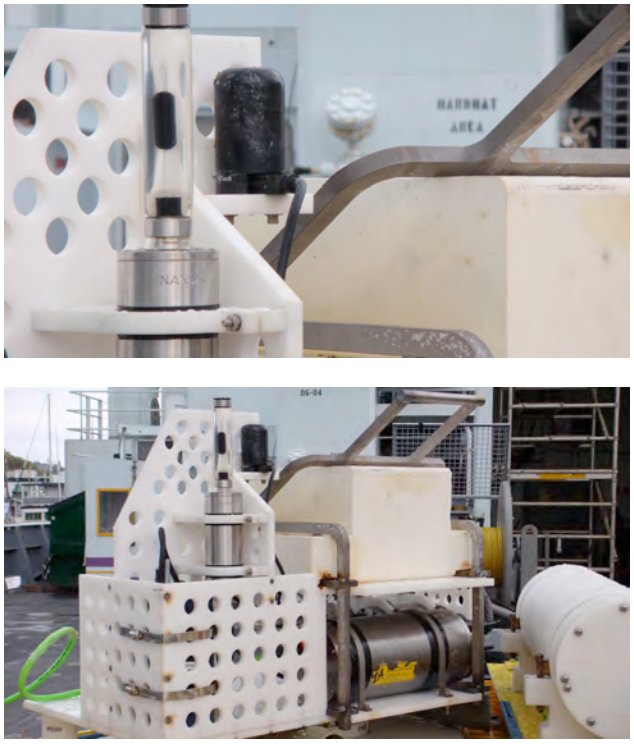

Fig. 4. (top) Detail of the hydrophone (small black cylinder inside the clear tube) and the WHOI micromodem transducer (larger black cylinder). (bottom) The complete instrument package on the deck of the R/V *Thompson* prior to deployment at the Seahurst Observatory; the micromodem electronics is strapped in the corner. The SIIM pressure case is visible with a yellow APL sticker. The CTDs and BB2F are behind the SIIM. The white block is syntactic foam to make the package near neutral buoyancy. The float secondary node is the Delrin cylinder to the right (all the connectors are on the hidden end).

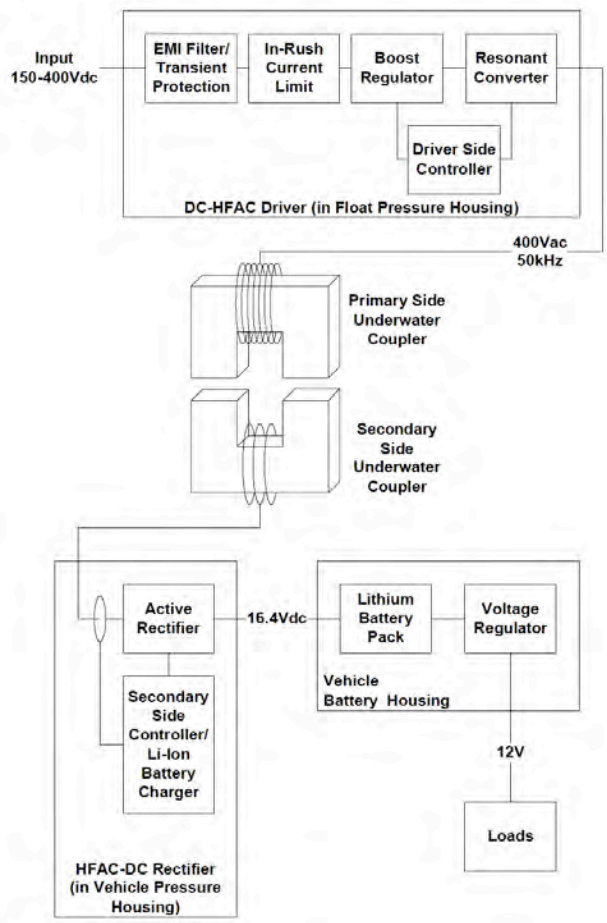

Fig. 5. Inductive Power System Block Diagram. A series resonant converter drives a constant frequency square wave voltage across the inductive coupler that is rectified and regulated on the secondary side.

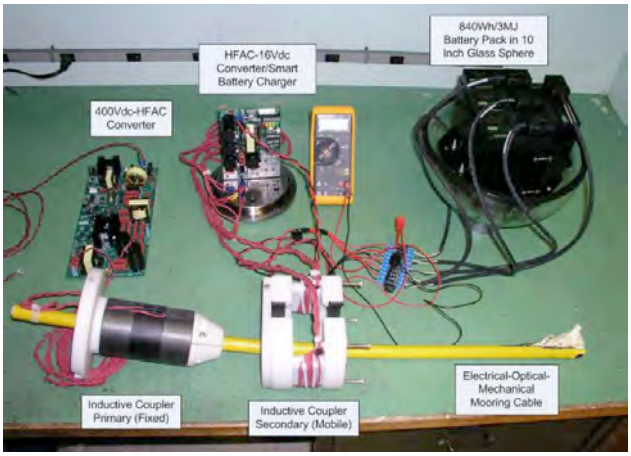

Fig 6. The inductive power system (IPS) components.

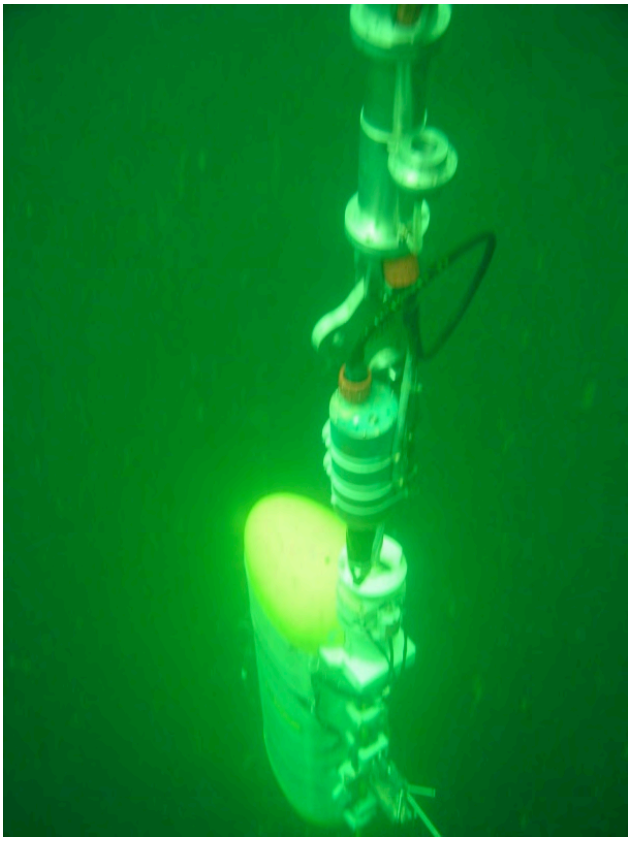

Fig. 7. (top) Deploying the MMP. The inductive power system primary is at the very top on the mooring cable, the secondary is on top of the profiler. The acoustic current meter has the 4 arms in the middle. The CTD sensors are wrapped in anti-fouling copper tape. (lower) The MMP on the mooring in Puget Sound in the docking position. One electro-optical converter is above the dock followed by a D-plate and the electro-mechanical swivel.

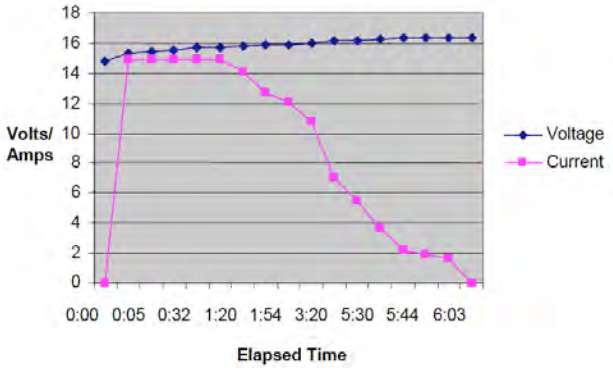

Fig. 8. Plot of the battery voltage and current during charging, measured at the battery.

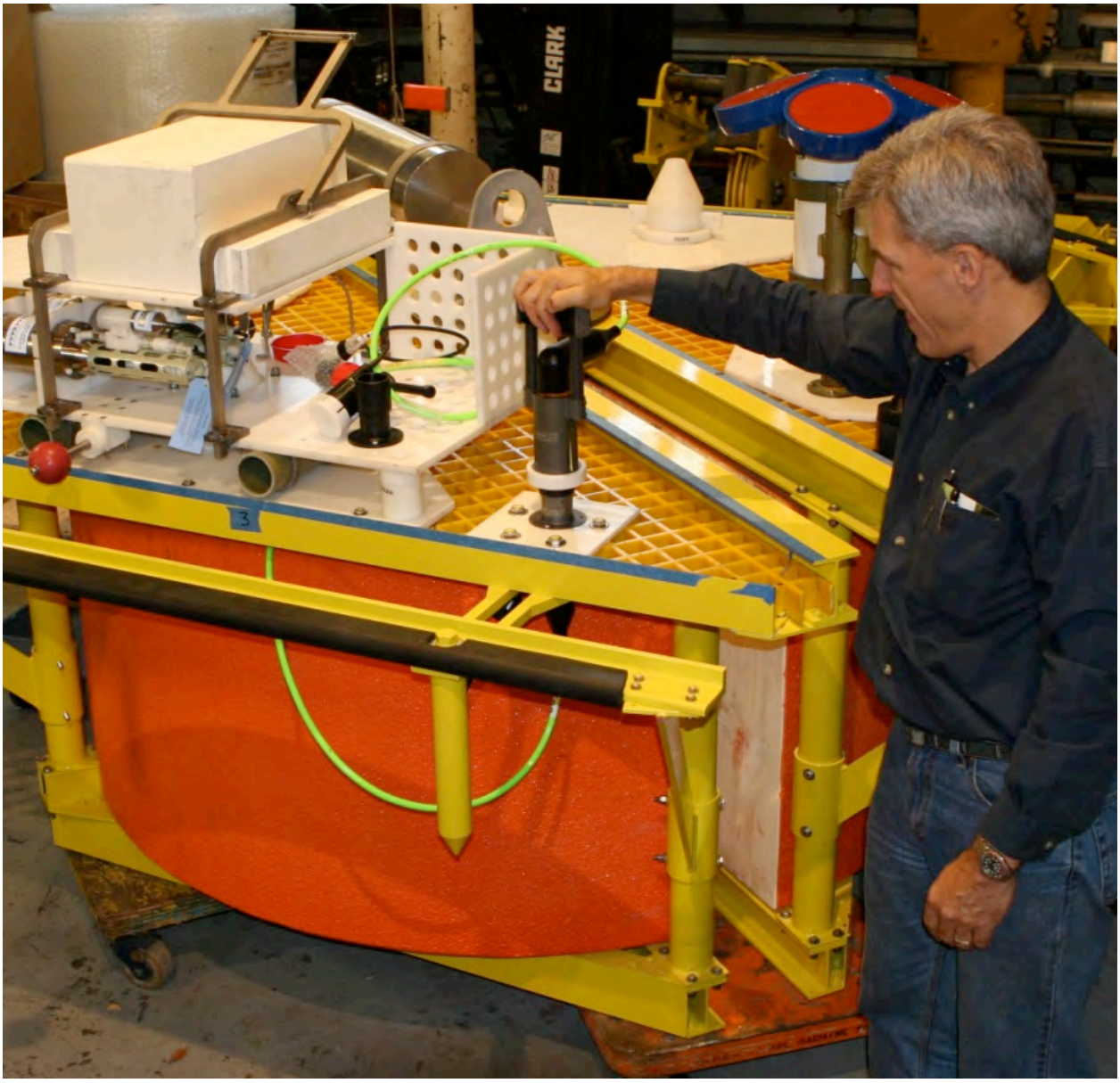

Fig. 9. The subsurface float. The instrument module with two CTDs is on the left; TM is plugging in the ROV mateable connector, connected to the secondary node in the left background. The ADCP it top right. A titanium post fits into the slot in the float.

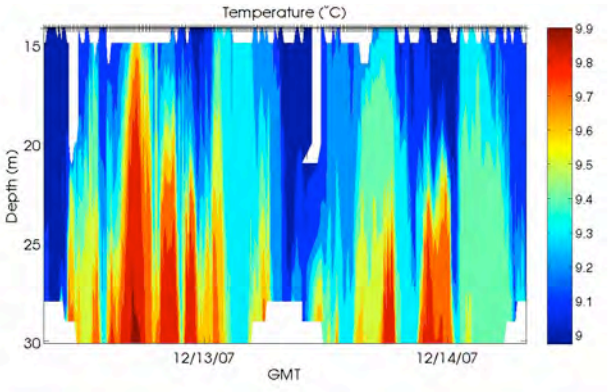

Fig 10. Temperature as a function of depth (vertical axis) and time (horizontal axis). Warm (and salty) bottom intrusions associated with tidal flow are clear.

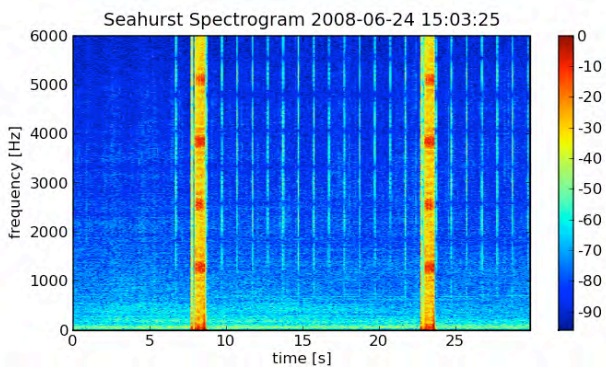

Fig. 11. Hydrophone spectrogram showing two strong modem signals (saturated, aliased here) and the ADCP transmissions at 1 second intervals.

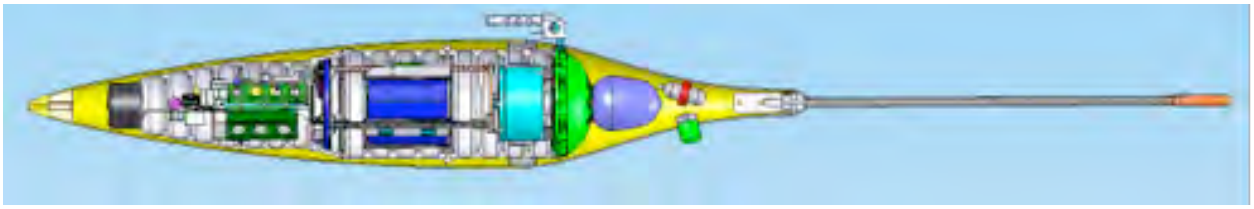

Fig. 12. The acoustic Seaglider. The hydrophone is in tail cone at the top, the acoustic modem transducer beneath it. The body contains (left to right) an acoustic emergency locator transponder/altimeter, electronics and low voltage batteries, high voltage batteries on a mass shifter for changing pitch and roll, buoyancy engine (oil pump) with internal and external oil bladder, and GPS and Iridium antenna.

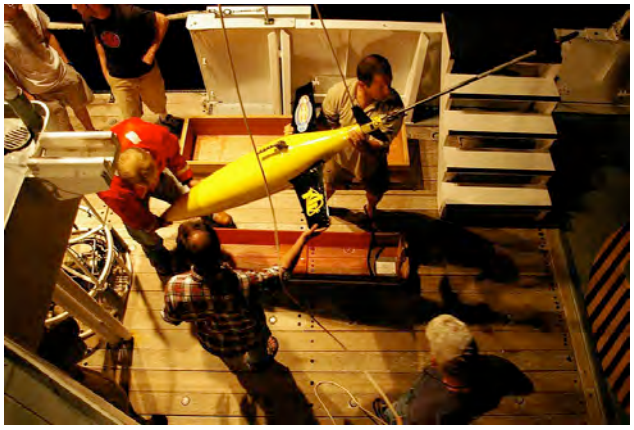

Fig. 13. Acoustic Seaglider being recovered after a Monterey Bay mission (courtesy J. Curcio).

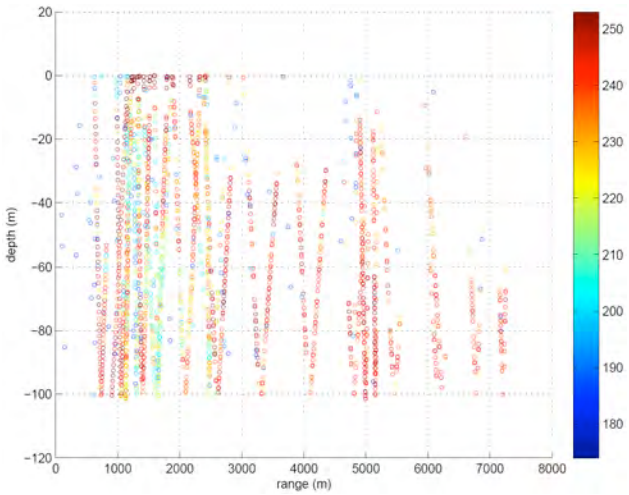

Fig. 14. Signal quality versus range and depth. Signal quality ranges from 253 (high signal-to-noise ratio) to 100 (low SNR). One glider is sitting on the bottom communicating with another glider making multiple dives. Data from Puget Sound tests conducted summer 2007.

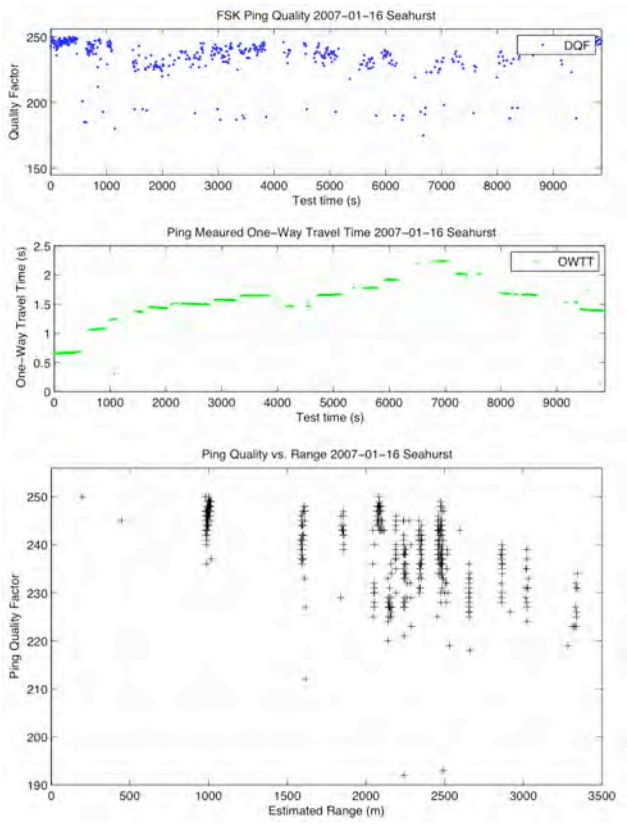

Fig. 15. Acoustic modem results from Seahurst tests: (top) signal quality versus time, (middle) travel time versus time, (bottom) quality versus range.

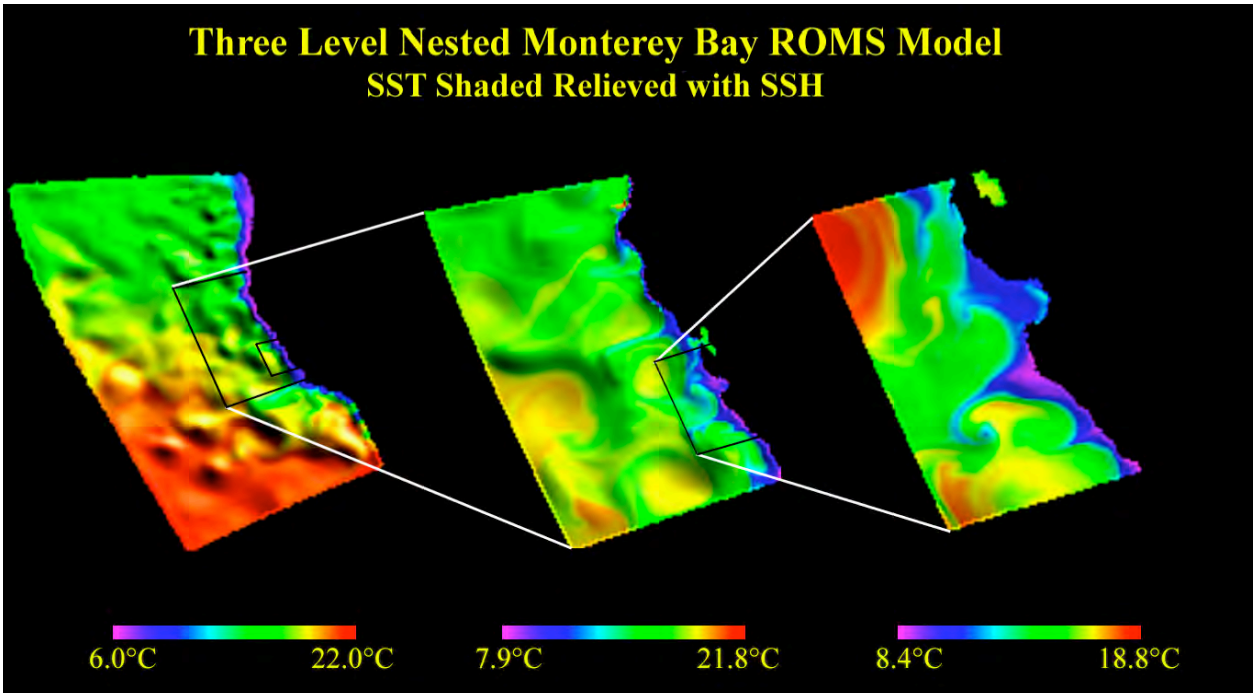

Fig. 16. Sea surface temperature as simulated by the three nested ROMS models with a spatial resolution of 15-km (left), 5-km (middle), and 1.5-km (right), respectively.

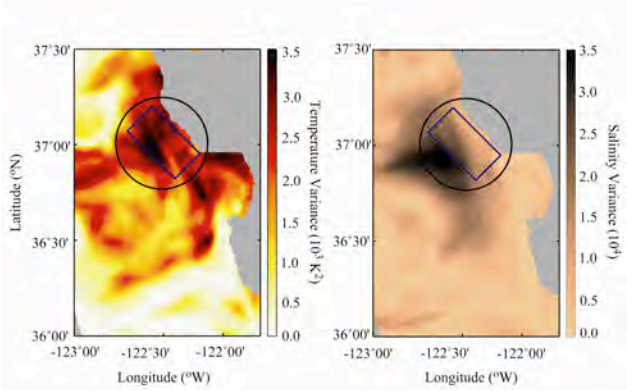

Fig. 17. ROMS-derived guidance aimed at improving a 1-day ROMS prediction within the blue rectangle region. Darker shading corresponds to preferred locations for sampling targeted observations of (A) temperature and (B) salinity.

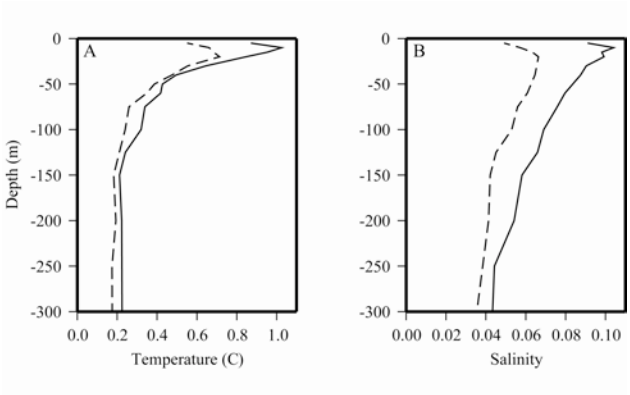

Fig. 18. ROMS reanalysis RMS errors in (A) temperature and (B) salinity before (solid line) and after (dashed line) the adaptive sampling deploying a glider following the ROMS derived guidance.